Supporting information for:

Barrierless Switching between a Liquid and Superheated Solid Catalyst During Nanowire Growth

*Christopher W. Pinion[1], David J. Hill[1], Joseph D. Christesen[1], James R. McBride[2], and James F. Cahoon[1]**

[1]Department of Chemistry, University of North Carolina at Chapel Hill, Chapel Hill, NC 27599-3290, United States, [2]Vanderbilt Institute of Nanoscale Science and Engineering, Vanderbilt University, Nashville, Tennessee 37235, United States

*Corresponding Author

Email: jfcahoon@unc.edu

1. Materials and Methods

1.1 Nanowire Growth

NWs were grown in a hot-walled chemical vapor deposition system using a quartz-tube furnace (Lindberg/BlueM Mini-Mite) at 390 °C and 40 Torr total pressure except when noted otherwise. The furnace temperature was calibrated against an external K-type thermocouple to ensure the temperature readings reflected the actual temperature within the furnace. Based on these calibrations, we are confident in the temperature to ± 5 °C. NWs were grown with 2.00 sccm SiH_4 (Voltaix), 200 sccm H_2 (Matheson 5N semiconductor grade), alternately 0.0 or 20.0 sccm PH_3 (Voltaix), and alternately 0.0 or 0.15 sccm HCl (Matheson semiconductor grade). NW segments grown with 20.0 sccm PH_3 are labeled n-type ("n") whereas segments with no PH_3 flow are labeled intrinsic ("i"). For NW growth, citrate-stabilized Au colloids of specific diameters (BBI International) were drop cast onto Si/SiO_2 substrates (University Wafer) functionalized with poly-L-lysine (Aldrich). NW growth was nucleated at 450 °C for at least 5 minutes and the temperature was then decreased (1 °C/min) to the process temperature of 390 °C. The temperature was held at 390 °C for at least eight minutes before initiating the liquid-solid switching process described in the main text. For temperature-dependent NW growth studies, all temperature changes were performed during n-type sections at a rate of 1 °C/min, and each set point temperature was allowed to stabilize for at least 2 minutes before encoding additional intrinsic or n-type segment for the determination of NW growth rates.

1.2 Nanowire Etching and Growth Kinetics Measurements

After completion of NW growth, NWs were mechanically transferred from the growth wafer to $Si/SiO_2/Si_3N_4$ substrates (Nova Electronic Materials) for wet-chemical etching in aqueous KOH solution (10 g KOH in 40 mL deionized water (18 MΩ) with a 20 mL surface

layer of isopropanol) at room temperature. The KOH etched was preceded by a 5 second etch in buffered hydrofluoric acid (Transene BHF Improved) to remove a native oxide layer on the NW, and the KOH etch was followed by a quench in dilute acetic acid. Typical etch times were 1 minute. Each VLS or VSS section of a NW at a particular growth temperature was encoded with at least two n-type segments and at least one intrinsic segment, which enabled reliable tracking of the growth's progress *ex situ* by counting the etched and unetched segments along the NW. The growth rate measurements presented in this work were taken from intrinsic segments.

1.3 Electron Microscopy and Elemental Mapping

Samples for electron microscopy were prepared by drop-casting NWs directly on to lacey-carbon TEM grids (Ted-Pella #01895). STEM imaging was performed on a Tecnai Osiris operating at 200 kV with a sub-nm probe (~5 Å) with a current of 1.5 nA (spot size 4, 3950k extraction voltage). Drift-corrected STEM-EDS maps were obtained using the Bruker Esprit software. The total collection times for each map were 15 minutes as longer collection times resulted in loss of drift correction at high magnification. STEM images were obtained before and after map acquisition to note any change in the sample. The instrument resolution is ~5 angstroms. However, the final resolution of the elemental map in Figure 3C is a convolution of the challenge of measuring the P signal, NW alignment relative to the electron beam, and the difficulty of drift correction on a featureless cylinder. Figure S2 depicts the raw P EDS map and EDS spectra. SEM imaging was performed with an FEI Helios 600 Nanolab dual beam system with an imaging resolution of less than 5 nm.

1.4 Thermodynamic Model of Catalyst-NW System

Equation 1 from the main text describes the ΔG associated with phase and compositional changes in the catalyst-NW system. The free energy change was calculated using published

thermodynamic data[1]. Specifically, the change in Gibbs free energy to create a given state when starting from the elemental solids was described using a simple substitutional model[1]:

$$\Delta G_f (n^L_{Au}, n^L_{Si}, T) = n^L_{Au}\, {}^oG^L_{Au} + n^L_{Si}\, {}^oG^L_{Si} + \ldots \\ \left(n^L_{Au} + n^L_{Si}\right)RT(x_{Si}\, ln(x_{Si}) + x_{Au}\, ln(x_{Au})) + \left(n^L_{Au} + n^L_{Si}\right)\Delta^E G, \quad \text{(S1)}$$

where n^L_{Au} is the moles of liquid Au, n^L_{Si} is the moles of liquid Si, T is the absolute temperature, ${}^oG^L_{Au}$ is the Gibbs free energy of formation for liquid Au, ${}^oG^L_{Au}$ is the Gibbs free energy of formation for liquid Si, R is the ideal gas constant, x_{Si} is the mole fraction of Si, x_{Au} is the mole fraction of Au, and $\Delta^E G$ is the excess Gibbs free energy, which is given by a Redlich-Kister polynomial of the form:

$$\Delta^E G = x_{Au} x_{Si} \sum_{v=0}^{n} (x_{Au} - x_{Si})^v\, L^{(v)}_{Au,Si}(T), \quad \text{(S2)}$$

where each coefficient, L, is a linear function of the temperature given by:

$$L^{(v)}_{Au,Si}(T) = a^{(v)}_{Au,\,Si} + b^{(v)}_{Au,\,Si}\, T, \quad \text{(S3)}$$

where the coefficients a and b, correspond to the excess enthalpy and entropy, respectively. The values of ${}^oG^L_{Au}$, ${}^oG^L_{Si}$, $a^{(v)}_{Au,\,Si}$, and $b^{(v)}_{Au,\,Si}$ were taken from ref. 26 in the main text.

1.5 Thermodynamic Model of Catalyst Solidification

For solidification, our model considers the nucleation and growth of a solid Au nanoparticle as the Si content in a 100 nm diameter hemispherical liquid alloy catalyst is depleted. As illustrated in Figure 4B of the main text, the solid particle is assumed to nucleate at the center of the catalyst-NW interface for simplicity. We calculate the change in Gibbs free energy to go from an undersaturated liquid alloy at the specified Si concentration to a liquid alloy and Au solid as a function of the solid nanoparticle radius.

The contributions from the various surface energies, γ_{sl}, γ_{lv}, and γ_{sv}, are also included in equation 1 from the main text, but are insignificant relative to the free energies associated with the changes in composition/phase[1-4].

To produce the plots in Figure 4B, we calculate the change in free energy as a function of solid particle size for a variety of starting Si concentrations in the liquid alloy using equation 1 from the main text with $m = -1$ and ignoring the surface term. This problem ultimately reduces to expressing n_{Au}^{L} as a function of the solid nanoparticle radius, r, then calculating $x_{Au}(r)$ and $x_{Si}(r)$ based on the initial amount of Si in the liquid alloy. For the simple hemispherical model we employed, this gives:

$$n_{Au}^{L}(r) = n_{Au}^{o} - \frac{2/3\pi r^3}{V_{m,Au}}, \tag{S4}$$

where n_{Au}^{o} is the initial amount of Au in the liquid catalyst and $V_{m,Au}$ is the molar volume of Au.

For each starting Si concentration, the amount of Au in the catalyst is the same, and for a given starting Si concentration the total amount of Au and Si is fixed. Thus, as the solid Au nanoparticle grows, the Si concentration in the liquid increases and returns the system closer to the liquidus concentration, which leads to a $\Delta G < 0$ for Si concentrations below ~15%. As depicted in Figure 4B, there exists a solid nanoparticle size for each starting concentration less than ~15% that produces a minimum in the ΔG vs. particle radius plot. This minimum corresponds to the Si concentration in the liquid alloy returning to the liquidus concentration. Once at the liquidus concentration, solidifying additional Au from the liquid supersaturates the alloy and increases the free energy of the system.

1.6 Thermodynamic Model of Catalyst Liquefaction

Our model of catalyst liquefaction considers the nucleation and growth of a liquid AuSi

cap on a solid Au nanoparticle. The Gibbs free energy was calculated using equation 1 from the main text with $m = 1$. The surface energies used to calculate $\Delta G_{surface}$, γ_{sl}, γ_{lv}, and γ_{sv}, were assigned their literature values of 0.25, 1.0 and 0.7 J/m^2, respectively[2-4]. As illustrated in Figure 4D of the main text, the liquid cap is assumed to nucleate at the tip of the catalyst for simplicity. We calculate the change in Gibbs free energy to go from a solid Au nanoparticle to a solid Au nanoparticle with a liquid alloy cap containing 18 atomic % Si of height, h, as a function of the liquid cap height and the temperature. Once again, this problem ultimately reduces to expressing n_{Au}^{L}, n_{Si}^{L}, and the various interfacial areas as a function of the liquid alloy cap height, h. The moles of Au and Si in the liquid cap are given by:

$$n_{Au}^{L}(h) = \frac{\pi h^2 (3R-h)}{3 V_{m\,Au}} x_{Au}\,, \tag{S5}$$

and

$$n_{Si}^{L}(h) = \frac{\pi h^2 (3R-h)}{3 V_{m,Si}} x_{Si}\,, \tag{S6}$$

where R is the catalyst radius, $V_{m,Au}$ is the molar volume of Au, x_{Au} is the mole fraction Au, $V_{m,Si}$ is the molar volume of Si, and x_{Si} is the mole fraction Si. Equation 2 from the main text describes how the interfacial areas scale with liquid cap height.

2. Supporting Figures

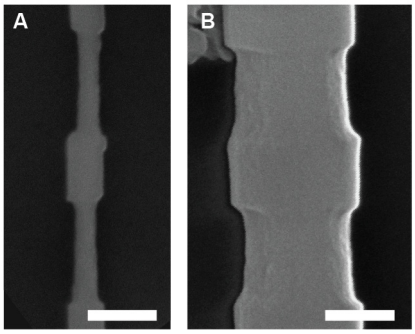

Figure S1. Representative NWs from VSS growth kinetics studies. SEM images of representative (**A**) ~50 nm and (**B**) ~150 nm diameter NWs used to determine the diameter-dependent VSS growth rates depicted in Figure 3A from the main text; scale bars, 100 nm. These specific ~50 and ~150 nm diameter NWs yielded growth rates of 2.5 ± 0.1 and 1.9 ± 0.1 nm/min, respectively.

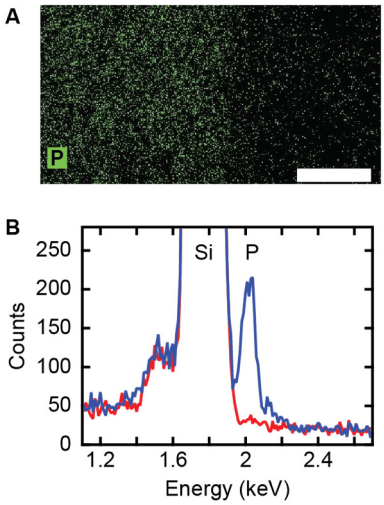

Figure S2. STEM EDS data. (**A**) Map of raw P counts (green) for the inset of Figure 3C; scale bar 6 nm. (**B**) EDS spectra showing the Si and P peaks from the heavily doped (blue) and 'intrinsic' (red) regions. The probe diameter during EDS measurement was ~5 Å.

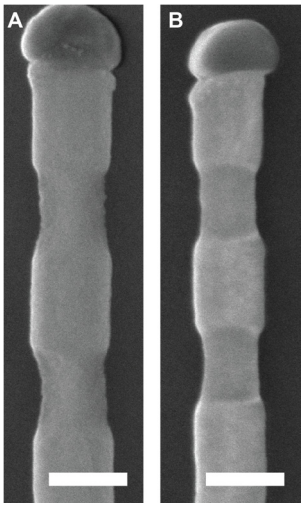

Figure S3. Absence of SLV etching under hydrogen atmosphere. SEM images of modulation-doped and etched Si NWs (**A**) without SLV etching and (**B**) with one hour of SLV etching (*i.e.* no SiH_4 in the reactor) at 390 °C; scale bars, 100 nm. The similarity of each image indicates the uptake process (*cf.* Figure 4A) is inhibited at these synthetic conditions.

References

(1) Chevalier, P. Y. A Thermodynamic Evaluation of the Au-Ge and Au-Si Systems. *Thermochim. Acta* **1989,** *141*, 217-226.

(2) Cognard, J. Adhesion to Gold: A Review. *Gold Bull.* **1984,** *17*, 131-139.

(3) Naidich, Y. V.; Perevertailo, V. M.; Obushchak, L. P. Density and Surface Tension of Alloys of the Systems Au-Si and Au-Ge. *Soviet Powder Metallurgy and Metal Ceramics* **1975,** *14*, 403-404.

(4) Naidich, Y. V.; Perevertailo, V. M.; Obushchak, L. P. Contact Properties of the Phases Participating in the Crystallization of Gold-Silicon and Gold-Germanium Melts. *Soviet Powder Metallurgy and Metal Ceramics* **1975,** *14*, 567-571.